

From antiferromagnet to altermagnet: the controllable spin source for MRAM

Cheng Song¹, Shixuan Liang¹, Hua Bai¹, Feng Pan¹, Aitian Chen² and Xixiang Zhang²

¹Key Laboratory of Advanced Materials, School of Materials Science and Engineering, Tsinghua University, Beijing 100084, China, songcheng@mail.tsinghua.edu.cn

²Physical Science and Engineering Division, King Abdullah University of Science and Technology, Thuwal 23955, Saudi Arabia, aitian.chen@kaust.edu.sa; xixiang.zhang@kaust.edu.sa

The generation of the spin current is fundamental to spin-orbit torque and the development of corresponding magnetic random access memory (MRAM). Compared with the conventional spin Hall effect (SHE), Néel vector-dependent spin current generation offers enhanced controllability for MRAM applications. By harnessing the out-of-plane spin polarization (σ_z) from antiferromagnetic SHE in Mn_2Au , we achieve field-free SOT switching of perpendicular magnetic tunnel junctions (pMTJs), enabling fully electrical writing and reading. For a non-relativistic counterpart, we utilized spin splitting torque in altermagnet RuO_2 , and also demonstrate a σ_z -enabled pMTJ, where spin polarization is aligned with the Néel vector. These three-terminal pMTJs operate at room temperature with a tunnel magnetoresistance ratio over 60%, lower critical current density, and faster, more efficient switching than conventional in-plane devices. These findings advance the application of unconventional spin current and support the development of high-density, low-power magnetic memory technologies.

Index Terms—antiferromagnet, altermagnet, magnetic tunnel junction, spin source

I. INTRODUCTION

THE generation of spin current is fundamental to spin-orbit torque (SOT), which enables higher endurance, higher switching speeds and lower energy consumption in magnetic random access memory (MRAM). Conventional spin Hall effect (SHE) is widely employed to generate spin current capable of inducing magnetization switching in adjacent ferromagnetic layers. However, in systems with perpendicular magnetic anisotropy, the orthogonality between the perpendicular magnetization and the in-plane spin polarization (σ_y) necessitates an external in-plane magnetic field to break the symmetry and achieve deterministic switching. This requirement poses a significant challenge for high-density memory applications. A promising strategy to overcome this limitation is the introduction of an out-of-plane spin polarization (σ_z), which emerges in spin sources with low crystal[1] or magnetic symmetry, including ferromagnets, antiferromagnets[2] and altermagnets[3], [4].

In this work, we utilize both the antiferromagnet Mn_2Au [5] and the altermagnet RuO_2 as spin sources to demonstrate σ_z -enabled three-terminal functional perpendicular magnetic tunnel junctions (pMTJs) with fully electrical writing and reading. Our devices exhibit a room-temperature tunnel magnetoresistance ratio exceeding 60%, along with a reduced critical current density and ultrafast, more efficient switching of perpendicular magnetization compared to conventional in-plane devices. Our findings advance the practical applications of unconventional spin polarization and pave the way for embedded memory and edge computing as the future magnetic memory.

II. GENERATION OF UNCONVENTIONAL SPIN POLARIZATION

In Mn_2Au (Fig. 1a), the magnetic sublattices exhibit local broken inversion symmetry. As shown in Fig. 1b, the emergence of σ_z depends on the alignment between the Néel vector \mathbf{n} and

the applied current \mathbf{J} — σ_z appears only when \mathbf{J} has a component parallel to \mathbf{n} . In this case, carrier spins (aligned with \mathbf{n}) are rotated out of plane by the spin-orbit field \mathbf{H}_{so} (purple arrows), which arises from the local symmetry breaking. Because both the carrier spins and \mathbf{H}_{so} are antiparallel between sublattices, a net σ_z is generated. Additionally, Mn_2Au also produces σ_y via the conventional SHE. Both σ_z and σ_y flow along the z-axis and exert unconventional spin-orbit torques on the adjacent ferromagnetic layer.

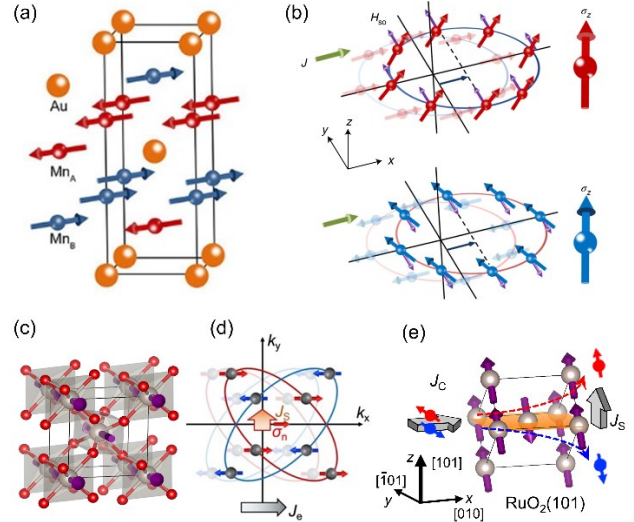


Fig. 1. Schematic of generating unconventional spin polarization in Mn_2Au and RuO_2 .

In RuO_2 , magnetic Ru atoms sit at the center of stretched octahedra formed by surrounding O atoms (Fig. 1c). Octahedra from opposite sublattices are related by rotational symmetry, generating alternating crystal potentials that lead to anisotropic magnetization densities and spin-split Fermi contours at $k_z = 0$. Due to this anisotropic spin band splitting, applying an charge current J_c along the $[010]$ axis shifts the Fermi contours, generating a transverse spin current J_s polarized along the Néel

vector, as shown in Fig. 1d[6]. For (101)-oriented RuO₂ films, a charge current along [010] induces a transverse, time-reversal-odd spin current along [100], with both the current and spin polarization containing out-of-plane components. As illustrated in Fig. 1e, this results in a σ_z spin current flowing along the z -axis, with spin polarization aligned with the Néel vector ([001]).

III. ELECTRICAL CONTROL OF PERPENDICULAR MTJ'S

The schematic and optical images of the σ_z -enabled pMTJ's are illustrated in Fig. 2a and 2b, respectively. Above the spin source channel, the device stack consists of a CoFeB free layer, an MgO barrier, and a CoFeB reference layer (the perpendicularly magnetized synthetic antiferromagnetic Co/Pt multilayers used to pin the reference layer are not shown). A Mo buffer layer is inserted beneath the free layer to enhance its perpendicular magnetic anisotropy and to facilitate efficient spin current transmission, owing to Mo's relatively long spin diffusion length.

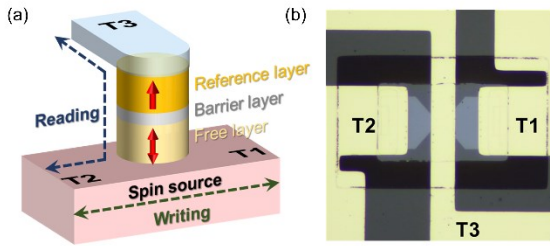


Fig. 2. Reading and writing in the σ_z -based pMTJ's.

A current applied between Terminal 1 (T1) and Terminal 2 (T2) flows through the spin source channel (writing path, indicated by the green dashed double arrow), generating both conventional spin torque via the SHE and z -polarized spin torque via antiferromagnetic SHE in Mn₂Au (or spin splitting torque in RuO₂). This enables deterministic switching of the free layer's perpendicular magnetization without an external magnetic field, completing the writing operation in the MTJ. Subsequently, a reading current of 1 μ A is applied between Terminal 3 (T3) and Terminal 2 (T2) to measure the tunnel magnetoresistance (TMR). Thus, the MTJ supports fully electrical writing and reading, enabling low-power SOT-MRAM operation.

The electrical performance of the Mn₂Au-based MTJ is characterized by TMR, defined as $(R_{\text{ap}} - R_{\text{p}})/R_{\text{p}} \times 100\%$, where R_{ap} and R_{p} are the resistances in the antiparallel and parallel configurations respectively. After applying a magnetic field of +0.15 T, the minor loop was measured as shown in Fig. 2a, indicating a TMR of 66%. We then demonstrate field-free SOT switching in the SOT-MTJ cell by sweeping the current from positive to negative and back. Using a parallel circuit model, the critical current density in Mn₂Au is estimated at 5.6×10^6 A/cm², an order of magnitude lower than conventional heavy-metal-based MTJ's. Notably, the high- and low-resistance states in Fig. 3b match those in Fig. 3a, confirming fully electrical SOT switching without an external field. Under an applied in-plane magnetic field, deterministic switching is also observed

with opposite polarity at -10 mT and $+10$ mT, as shown in Fig. 3c.

RuO₂-based pMTJ was characterized similarly. We demonstrate all-electrical control of pMTJ using RuO₂ writing channel along the [010] axis. Fig. 2d shows the minor loop of tunnel resistance versus $\mu_0 H_z$ for this device. When an applied field $\mu_0 H_x$ of ± 10 mT, current pulses induce magnetization switching of the free layer, causing TMR changes (Fig. 2f). More importantly, deterministic switching driven by current pulses was achieved without any external field $\mu_0 H_x$ as shown in Fig. 2e, with the critical switching current density is below 1×10^7 A/cm².

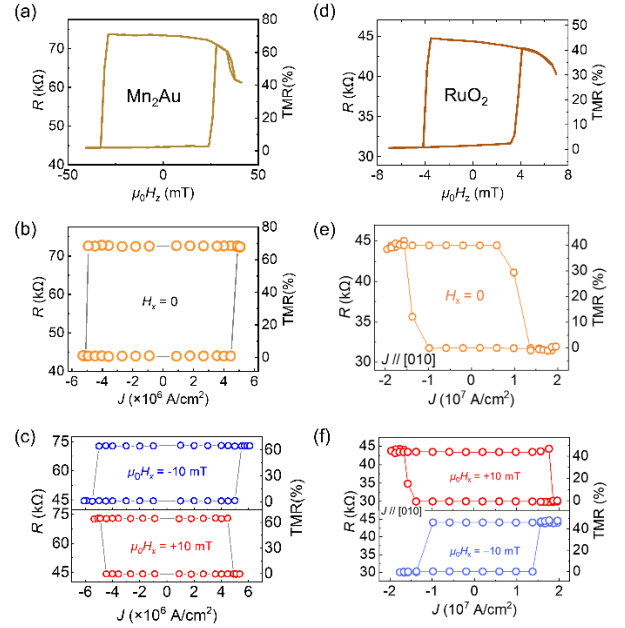


Fig. 3. Reading and writing in the σ_z -based pMTJ's.

REFERENCES

- [1] D. MacNeill, G. M. Stiehl, M. H. D. Guimaraes, R. A. Buhrman, J. Park, and D. C. Ralph, "Control of spin-orbit torques through crystal symmetry in WTe₂/ferromagnet bilayers," *Nat. Phys.*, vol. 13, no. 3, pp. 300–+, 2017, doi: 10.1038/NPHYS3933.
- [2] X. Chen *et al.*, "Observation of the antiferromagnetic spin Hall effect," *Nat. Mater.*, vol. 20, no. 6, pp. 800–804, 2021, doi: 10.1038/s41563-021-00946-z.
- [3] C. Song *et al.*, "Altermagnets as a new class of functional materials," *Nat. Rev. Mater.*, 2025, doi: 10.1038/s41578-025-00779-1.
- [4] Z. Zhou *et al.*, "Manipulation of the altermagnetic order in CrSb via crystal symmetry," *Nature*, vol. 638, no. March 2024, 2025, doi: 10.1038/s41586-024-08436-3.
- [5] S. Liang *et al.*, "Field-Free Perpendicular Magnetic Memory Driven by Out-of-Plane Spin-Orbit Torques," *Adv. Funct. Mater.*, vol. 2417731, pp. 1–8, 2024, doi: 10.1002/adfm.202417731.
- [6] H. Bai *et al.*, "Observation of Spin Splitting Torque in a Collinear Antiferromagnet RuO₂," *Phys. Rev. Lett.*, vol. 128, no. 19, p. 197202, 2022, doi: 10.1103/PhysRevLett.128.197202.